

Article

Mechanical Behaviour of Steel Slag–Rubber Mixtures: Laboratory Assessment

Rubens Alves ^{1,2,*} , Sara Rios ¹ , Eduardo Fortunato ³ , António Viana da Fonseca ¹ 
and Bruno Guimarães Delgado ¹

¹ CONSTRUCT-GEO, Faculty of Engineering, University of Porto, 4200-465 Porto, Portugal

² Federal Institute of Education, Science and Technology of Rio Grande do Norte (IFRN), Natal 59015-300, Brazil

³ Transportation Department, National Laboratory for Civil Engineering (LNEC), 1700-066 Lisboa, Portugal

* Correspondence: rubens.alves@ifrn.edu.br

Abstract: Slags and rubber from end-of-life tires represent a liability to the steel and tire industry, causing economic and environmental problems that are difficult to manage. Transport infrastructures can use these industrial by-products instead of extracting natural raw materials, but the adequate mechanical performance of the materials needs to be assured. This paper addresses the mechanical behaviour of slag–rubber mixtures in the laboratory with CBR, monotonic and cyclic triaxial tests. In addition, light falling weight deflectometer tests were also performed in a physical model. The results were analysed to meet technical specifications from Brazil, Portugal and Australia using railway sub-ballast layers, capping layers or road pavement layers as the base and sub-base to identify the applicability range of slag–rubber mixtures for transport infrastructures. Concerning the analysed parameters, it was demonstrated that slag–rubber mixtures can show resilient behaviour and strength adequate for the support layers of transport infrastructures provided that the rubber content is below 5% in weight and that the slag is milled to comply with the grain size distribution ranges available in the technical specifications of the cited countries.

Keywords: CBR; triaxial tests; resilient modulus; industrial by-products; physical model



Citation: Alves, R.; Rios, S.;

Fortunato, E.; Viana da Fonseca, A.;

Guimarães Delgado, B. Mechanical

Behaviour of Steel Slag–Rubber

Mixtures: Laboratory Assessment.

Sustainability **2023**, *15*, 1563. [https://](https://doi.org/10.3390/su15021563)

doi.org/10.3390/su15021563

Academic Editor: Fausto Cavallaro

Received: 11 October 2022

Revised: 12 December 2022

Accepted: 6 January 2023

Published: 13 January 2023



Copyright: © 2023 by the authors.

Licensee MDPI, Basel, Switzerland.

This article is an open access article

distributed under the terms and

conditions of the Creative Commons

Attribution (CC BY) license ([https://](https://creativecommons.org/licenses/by/4.0/)

[creativecommons.org/licenses/by/](https://creativecommons.org/licenses/by/4.0/)

[4.0/](https://creativecommons.org/licenses/by/4.0/)).

1. Introduction

In Portugal, electric arc furnace slags have been used as aggregates for construction, being dense, stiff, clean and resistant to abrasion. Laboratory tests, corroborated by full-scale field trials, have demonstrated that these steel slags have better mechanical properties (stiffness and resistance against permanent deformation) than standard base course materials. In addition, leaching and lysimeter tests have not revealed any environmental or public health risks [1]. More recently, this material has been studied as an alternative aggregate for railway ballast, demonstrating enhanced performance under the higher loads of heavy-haul trains [2]. This is in agreement with other studies, including both experimental evaluations and numerical modelling of the performance of coarse unbound materials containing steel slag [3,4].

Rubber from end-of-life tires can be reused as a whole or after shredding in different applications as specified in ASTM D6270 [5], benefiting from its resilient properties. According to Downs et al. [6], scrap rubber tires do not pollute ground water tables.

The different applications for slags and rubber contribute to reducing the amount that is landfilled or stockpiled, which has associated economic and environmental costs. Moreover, the use of these industrial by-products in transportation infrastructures avoids the extraction of natural raw materials, benefiting from all the advantages of a circular economy [7,8].

Several research studies have been conducted on the properties of scrap tires when mixed with sand, such as density, compactness, compressibility, stiffness and shear strength.

Mashiri et al. [9] considers that sand–rubber’s behaviour is mostly influenced by the rubber content: for a low rubber content, the addition of rubber increased the shear strength, initial tangent modulus and dilatancy, while for a higher rubber content, the opposite occurred, leading to an optimum point that the authors found to be around 35% (mass proportion). Fu et al. [10] also highlighted that the size and aspect ratio of rubber particles has a significant influence in the mixture shear behaviour. While shreds and larger chips typically increase the peak strengths (e.g., [11,12]), smaller chips, crumbs or granules often either have no effect on the strength or a negative one (e.g., [13–15]).

Sand and gravel–rubber mixtures have been studied in terms of their cyclic and dynamic properties for vibration isolation purposes [16–20], for railway ballast mixtures to reduce particle breakage and increase durability [21–25], and for resilient behaviour evaluation for their application in ballast and sub-ballast layers [26,27].

However, analyses of slag–rubber mixtures’ behaviour are still limited [28,29]. The idea of using two industrial by-products instead of one represents a significant advance towards a circular economy. Transport infrastructures use a great amount of raw materials and are therefore a convenient application for industrial by-products. For this purpose, thorough studies are required to assure that these alternative materials have the necessary mechanical performance to be used in transportation infrastructures.

Steel slags have a complex morphology [30,31] that affects the interlocking between particles. As they are very dense and strong, the particle breakage is expected to be reduced [32], but the contact stress may be significant. The introduction of rubber may reduce those contact stresses, reducing the stiffness and increasing the energy absorption capacity [33]. For this purpose, triaxial compression and cyclic triaxial tests were performed on slag–rubber mixtures compacted on the optimum point of a modified Proctor compaction curve. In addition, a physical model has been prepared which enables the application of the original grain size distribution curve, as well as the execution of light weight deflectometer (LWD) tests. These tests are economic and fast, enabling stiffness evaluations for a large number of points, as well as more representative of the dynamic action existing in a transport infrastructure [34–36].

2. Materials and Methods

2.1. Materials

The steel slag used in this study was collected in the National Steel Industry of Maia (SN Maia), part of MEGASA group, close to the city of Porto (Portugal). The chemical composition of this slag obtained by X-ray fluorescence is presented in Table 1 and the respective oxides are presented in Figure 1. The main elements are iron, calcium and silica whose corresponding oxides comprise almost 70% of the total composition. The amount of calcium and magnesia oxides can generate swelling problems due to their hydration, which creates calcium and magnesia hydroxides. However, these slags undergo an industrial process, as described in [1], which enables them to be classified by European CE marking as ‘Inert Steel Aggregate for Construction’ for use in civil engineering works and road construction.

Table 1. Chemical composition the slag obtained by X-ray fluorescence.

Elements	Chemical Composition (%)
Si	14.1
Ca	26.3
Mg	7.6
Al	8.5
Fe	29.2
Mn	6.3
Cr	3.6
Others	4.4

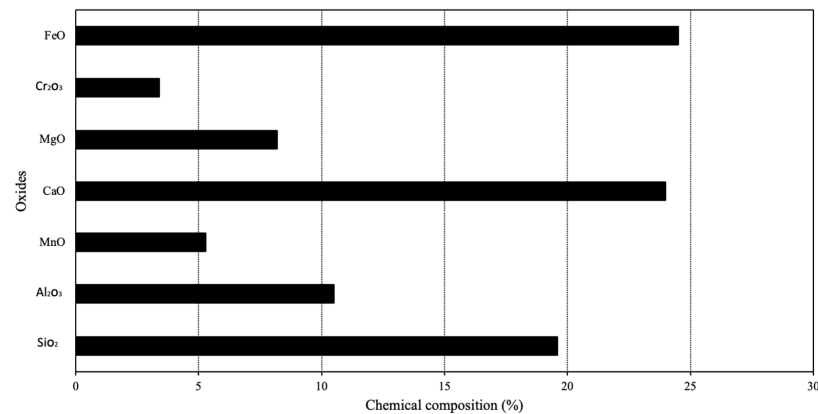


Figure 1. Slag chemical composition.

The slag particle size distribution (PSD) when it comes from the steel industry is presented in Figure 2, as original PSD. Its main properties are summarised in Table 2, together with the reference values according to EN 13,242 [37]. The lack of fine particles is its major disadvantage, as most technical specifications associated to the application of this material in the unbound granular layers of transport infrastructures require 4–8% to be fine (particles < 0.063 mm) [38]. In Figure 2 shows the particle size distribution range defined by the Portuguese specification for sub-ballast layers [38], which is similar to the specification for road base and sub-base layers. In order to comply with this specification, a new particle size distribution was defined (identified in Figure 2 as selected PSD) and the material was milled in a ball mill. The amount retained in each sieve for the selected PSD was obtained according to Equation (1) using an n value of 0.38. This distribution allows a high level of compaction according to [39], which was corroborated by the Proctor compaction tests presented below.

$$p = 100 \left(\frac{d}{D} \right)^n \quad (1)$$

where:

p —% of material passed on the sieve with mesh size d ;

D —maximum particle size;

n —parameter generally assumed to be close to 0.35 to obtain the maximum density.

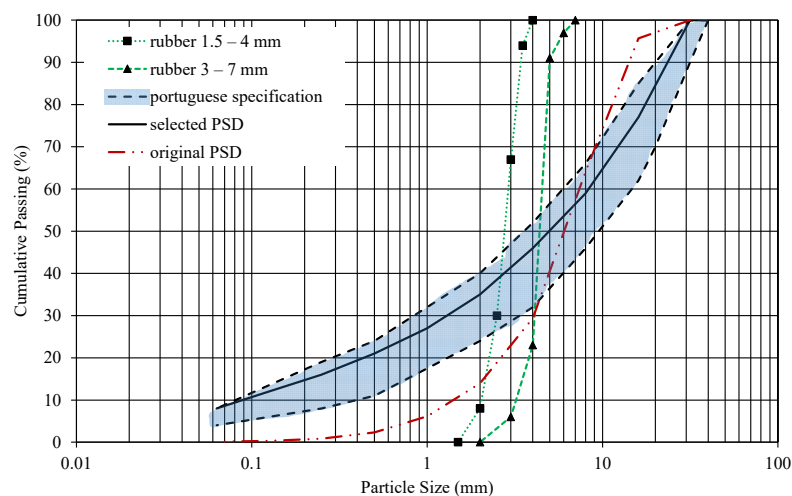


Figure 2. Slag and rubber particle size distributions (PSD) as well as the upper and lower bounds defined by the Portuguese specification [38].

Table 2. Slag parameters in the original PSD.

Parameters		Standard	Reference Values (EN 13,242 [35])	Average Values
Fines (%)		NP EN 933-1	≤5	0.9
Flakiness index		NP EN 933-3	≤20	2.2
Shape index		EN 933-4	≤20	4.2
Los Angeles index (%)		EN 1097-2	≤25	17.5
Particle's density (g/cm ³)	Impervious particles	NP EN 1097-6	3.58	3.59
	Dry particles	NP EN 1097-6	3.39	3.44
	Saturated particles	NP EN 1097-6	3.44	3.48
Water Absorption (%)		NP EN 1097-6	≤1.6%	1.2
Sulphur (%)		EN 1744-1	≤1	0.1
Volumetric swelling (%)		UNE EN 1744-1:2010 + A1:2013		0.15

The material in the selected PSD is considered a well-graded gravel with silt (GW-GM) according to the Unified Classification System [40], and the main geotechnical properties are summarized in Table 3.

Table 3. Geotechnical properties of the slag in the selected PSD.

Parameters	Values
Plastic Limit	NP
Liquid Limit	N/A
D ₅₀	4.00 mm
Specific gravity	3.53
Fines fraction (sieve N° 200)	8.00%
Uniformity Coefficient	100
Curvature Coefficient	2.25

NP—non plastic; N/A—not applicable.

The rubber used in this work results from mechanical shredding of end-of-life tires that are provided by GENAN©. This material is free from metallic wires and its particles range between 1.5 and 7 mm as seen in Figure 2, being classified as granulated rubber according to ASTM D6270 [5], with the properties indicated in Table 4.

Table 4. Rubber parameters.

Parameters	Test Method	Values
Specific gravity	ASTM D 1817-06(2016)	1.160
Bulk density	EN 1097-3 (1998)	0.395 g/cm ³
Polymer content	ISO 9924-3 (2009)	≥40%

2.2. Testing Procedures

The CBR tests as well as the monotonic and cyclic triaxial tests were performed on the slag–rubber mixtures using the selected PSD for the slag. When the rubber is added, the slag is replaced by rubber between 1.5 and 7 mm, so that the PSD remains unchanged (Figure 3a). Both materials were manually mixed until a homogeneous mixture was obtained, and then water was added to obtain the optimum moisture content.

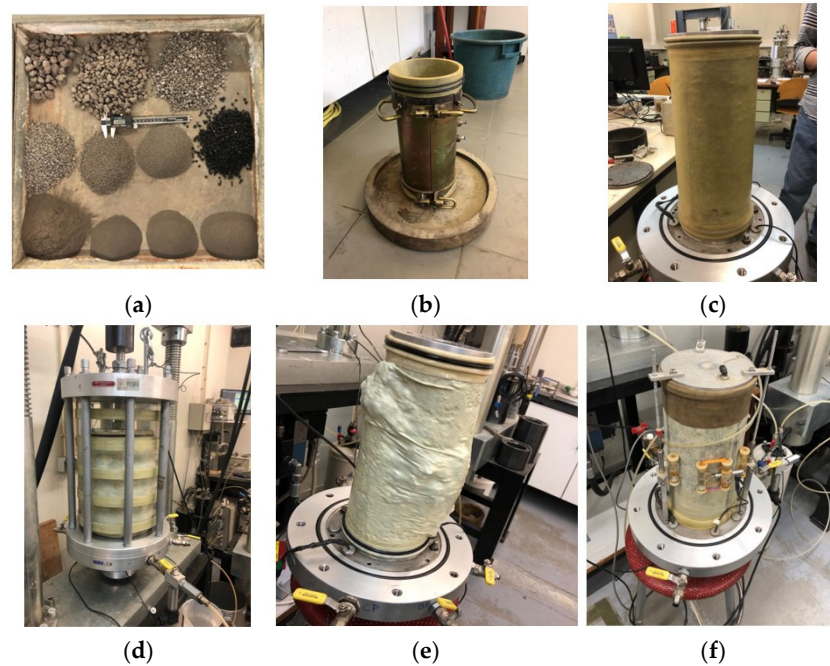


Figure 3. Test procedures: (a) different particles sizes; (b) mould with membrane inside for triaxial test; (c) specimen after compaction; (d) triaxial cell; (e) specimen after triaxial compression test; (f) specimen with internal instrumentation.

Compaction was performed using a vibrating hammer adapted for this specific purpose with a rod coupled with a 148 mm diameter disc. As demonstrated by Fortunato et al. [41], vibrocompaction is more adequate for granular materials, better reproducing the energy transmitted by the roll compactors in the field, in contrast to Proctor dynamic compaction, which tends to break the particles. For each layer of 50 mm thickness, 1 min of vibratory compaction was performed.

Specimens with rubber contents (Rb) of 0%, 2.5%, 5%, 7.5% and 10%, defined as mass ratios between the rubber and slag, were prepared on the optimum compaction point. These percentages were selected because [26,42] have shown that values above 10% are not adequate for infrastructures layers.

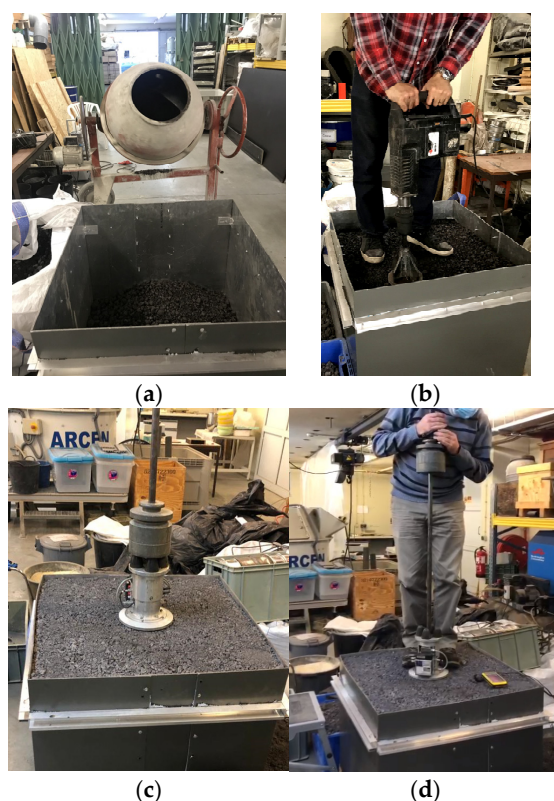
The specimens for the triaxial tests were moulded into a 300 mm high (plus 50 mm extension), 150 mm diameter mould so that the diameter of the specimen was 5 to 6 times larger than maximum particle dimension (31.5 mm) [43]. The mould and the compacted specimen are shown in Figure 3b,c. The consolidation phase took at least 12 h (Figure 3d) to allow for full dissipation of excess pore pressures. For the monotonic tests, a strain rate of 0.2 mm/min was applied by a 100 kN load frame, and a shear plane failure was formed approximately after the peak, which is typical of dense materials, as illustrated in Figure 3e.

The cyclic triaxial tests followed method B of EN 13286-7 [44] (constant effective confining stress), comprising a conditioning of 20,000 cycles with $\sigma'_3 = 70 \text{ kPa}$; $q = 340 \text{ kPa}$ and the load stages indicated in Table 5. in terms of effective confining stress (σ'_3) and maximum deviatoric stress (q_{max}). The applied confining stress was considered effective, because the magnitude of suction was almost insignificant for these materials and the generated excess of pore pressure rapidly dissipated. Schulz-Poblete et al. [42] have studied the influence of suction measured with tensiometers in sub-ballast material through box tests and concluded that suction was small (<10 kPa) or absent and did not play a significant role in material's behaviour. A cyclic sinusoidal load was applied with a frequency of 1 Hz, oscillating between a small deviatoric stress at around 5 kPa (q_{min}) and a maximum deviatoric stress (q_{max}). Internal instrumentation was used in these tests with 4 linear variable differential transducers (LVDT) (3 axial and 1 radial), providing more accurate resilient modulus, as can be seen in Figure 3f.

Table 5. Stress levels applied in the cyclic triaxial tests.

Constant Confining Stress, σ'_3 (kPa)	q_{\max}/σ'_3
20	1.50; 2.50; 4.00; 5.75
35	1.43; 2.29; 3.29; 4.29; 5.71
50	1.60; 2.30; 3.00; 4.00; 5.60
70	1.64; 2.14; 2.86; 4.00; 4.86
100	1.50; 2.00; 2.80; 3.40; 4.00
150	1.33; 1.87; 2.27; 2.67; 3.17

Physical models with dimensions of $0.8 \times 0.8 \times 0.64$ m (Figure 4a) were built to assess the mechanical behaviour of the slag–rubber mixtures on a larger scale in comparison with triaxial tests. For this purpose, the original PSD for the slag (Figure 2) was used. On the bottom of the model, two layers of slag with 10 cm thicknesses were compacted to act as a foundation material and to avoid the effect of the bottom boundary. Then, the upper part of the model was compacted in seven layers of 6 cm. Three models were built by varying the upper part, which had different rubber contents of 0%, 2.5% and 5%. Compaction was always performed with a vibrating hammer (Figure 4b). On the three models, the dynamic stiffness modulus was measured with a light weight deflectometer (LWD) with a plate 200 mm in diameter (Figure 4c,d) to avoid the influence of the foundation material, considering that the depth of the stress bulb was twice the diameter of the plate. The test was performed on the centre of the model to avoid boundary effects and the geophone where the deflections were measured was located in the centre of the plate, as done previously by [45].

**Figure 4.** Tests on the physical model: (a) details of the box and mixer; (b) compaction with adapted vibrating hammer; (c,d) measuring the stiffness modulus with LWD test.

To better understand the testing sequence, Figure 5 shows a flowchart representing the steps followed in this research study.

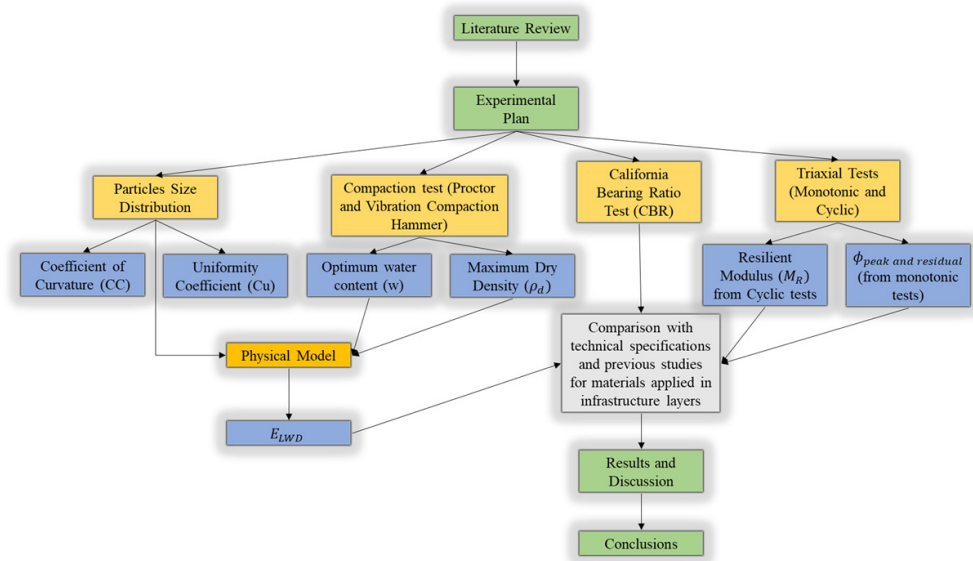


Figure 5. Flow chart of this study.

3. Results and Discussion

3.1. Compaction Properties

Figure 6 shows the variation in the dry density with the water content obtained by the modified Proctor [46] test and the vibrating hammer for the slag with the selected PSDs. The same figure also presents information regarding the different slag–rubber mixtures (made with the slag with the selected PSDs) performed with the vibrating hammer. As observed by [35], in coarse materials with a poor quantity of fines, the compaction curve is not well defined, and it is difficult to evaluate the maximum dry unit weight and optimum water content. The slag dry density is similar with both the vibrating hammer and modified Proctor, although the vibrating hammer allowed for a slightly higher maximum dry unit weight since granular materials compact better with vibration. In all the mixtures, the higher dry density values occurred when the material was dry or almost saturated, corroborating the results found by [47].

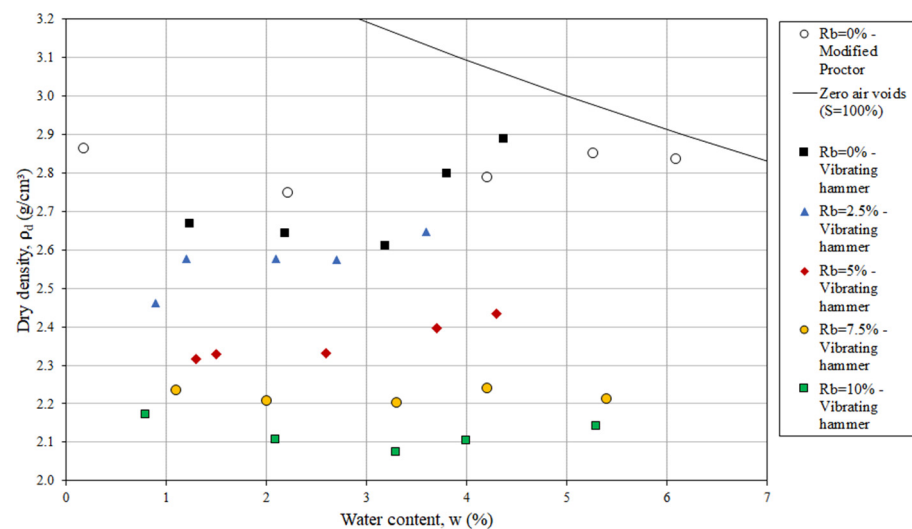


Figure 6. Dry density with water content for the slag on the selected PSD mixed with various rubber contents (Rb). NOTE: The zero air voids line corresponds to the compaction of ISAC without rubber (Rb = 0%) performed on modified Proctor.

While 4% of the water content presented slightly higher dry densities due to particle lubrication, the water contents higher than 4% resulted in drainage during compaction. For this reason, all the specimens for monotonic and cyclic triaxial and CBR tests were moulded with the same water content of 4% to avoid the influence of water content variation on the mixture behaviour. The moulding dry unit weight was the maximum value obtained for each rubber content. For the preparation of the three physical models, the slag on the original PSD mixed with rubber was compacted at an optimum water content of 3% and at a maximum dry density depending on the rubber content (Figure 7).

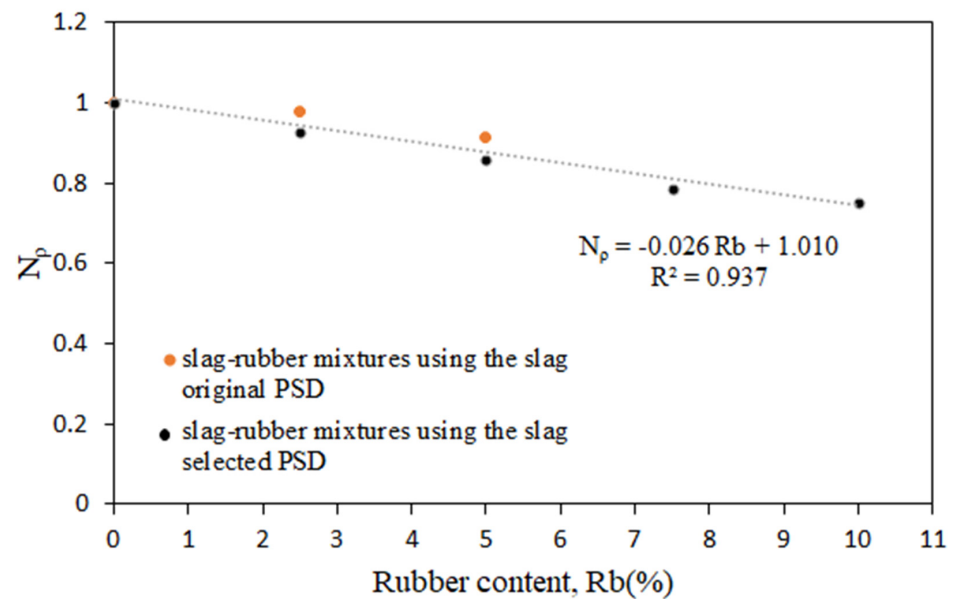


Figure 7. Normalised dry unit weight for the slag on the selected and original PSD with various rubber contents (Rb).

Figure 7 shows, for each rubber content, the moulding dry unit weight obtained in the compaction test for each mixture normalised by the moulding dry unit weight of the slag without rubber (N_p). The normalised dry densities of the slag–rubber mixtures are presented for both the selected PSD and for the original PSD. A clear linear relation was obtained for the data corresponding to both cases. Besides the different PSDs, the normalized dry density followed the same trend with rubber. Although it was expected that the increase in the quantity of rubber would cause a reduction in the dry density due to the lower unit weight of the rubber grains (Tables 3 and 4), such a clear linear relation can be very useful when estimating the mixture dry density, which depends on the rubber content.

In the past, CBR values were one of the most important parameters present in the specifications for granular materials for transport infrastructures. For this reason, this parameter is still in most technical documents, although other parameters, such as the resilient modulus, are gaining importance for design purposes. Comparing the specifications used in different countries, it becomes clear that while Portugal and Brazil have a single CBR limit applicable for sub-base or sub-ballast layers, Australia distinguishes the CBR values depending on the location of the material. Moreover, Australia requires higher CBR values than Portugal and Brazil for the same layer.

Figure 8 presents the CBR values obtained for the slag–rubber mixtures prepared on the selected PSDs. A rapid decrease with the increase in rubber content is observed, indicating that the rubber has a very important influence on the mixture’s mechanical behaviour. A small increase of 2.5% in the rubber content (from 0% to 2.5%) reduced the CBR values to half of the original value. In contrast, for higher rubber contents, the increment of rubber has a smaller impact on the CBR values, as the behaviour is already controlled by the rubber particles instead of the slag grains. This demonstrates that for higher percentages of rubber, there is more rubber–rubber contact, decreasing the strength

of the mixture. However, for mixtures with rubber contents less than 7.5%, the CBR values are still within the limits recommended in the Brazilian and Portuguese technical specifications for unbound layers in transport infrastructures.

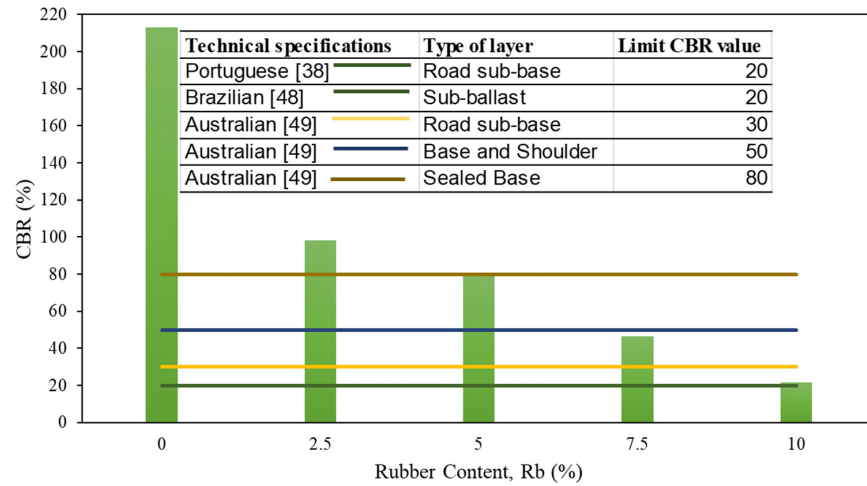


Figure 8. CBR values for different rubber contents (Rb) and acceptable limits according to [38,48,49].

3.2. Stress–Strain Behaviour

Figure 9 presents the stress–strain curves obtained in monotonic triaxial compression tests for the different slag–rubber mixtures, in terms of the deviatoric stress ($q = \sigma_1 - \sigma_3$) normalised by the mean effective stress ($p' = \frac{\sigma_1 + 2\sigma_3}{3}$) and axial deformation (ϵ_a).

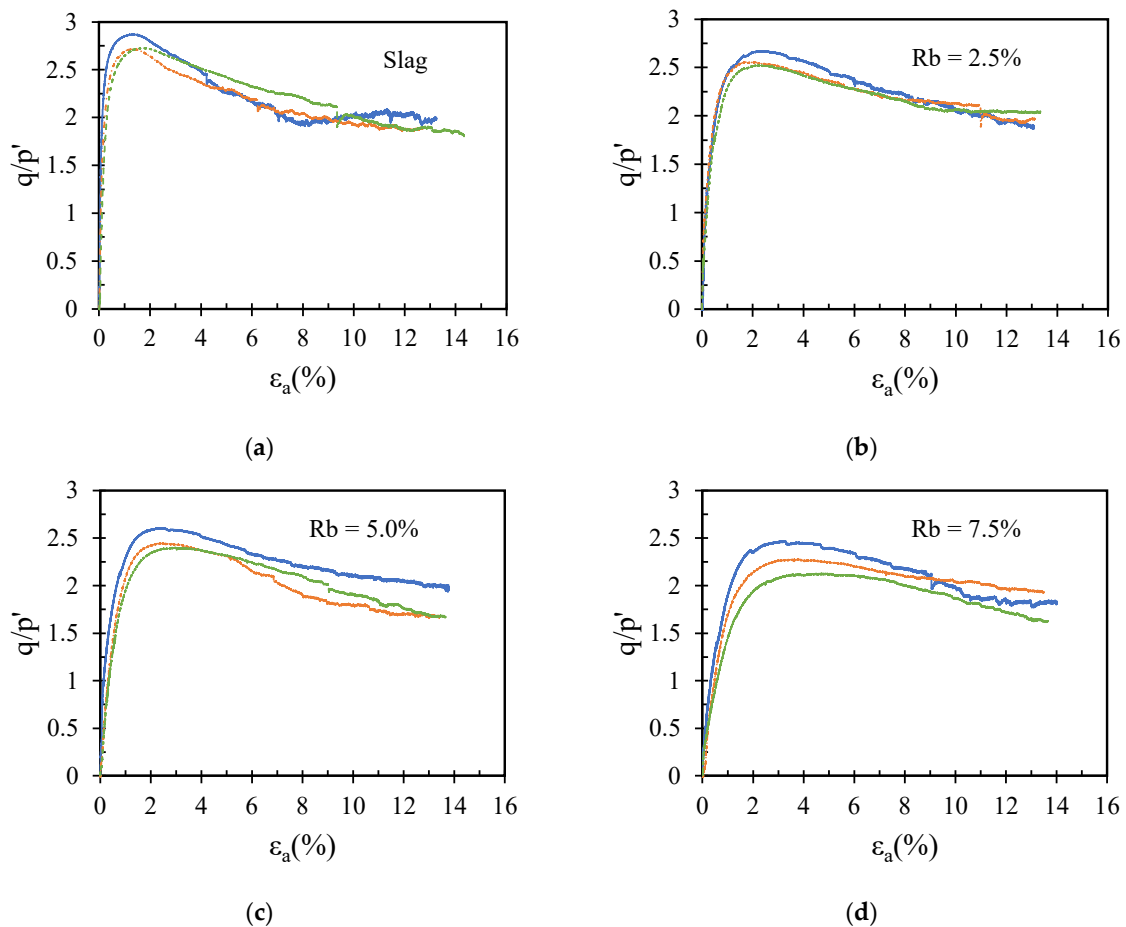


Figure 9. Cont.

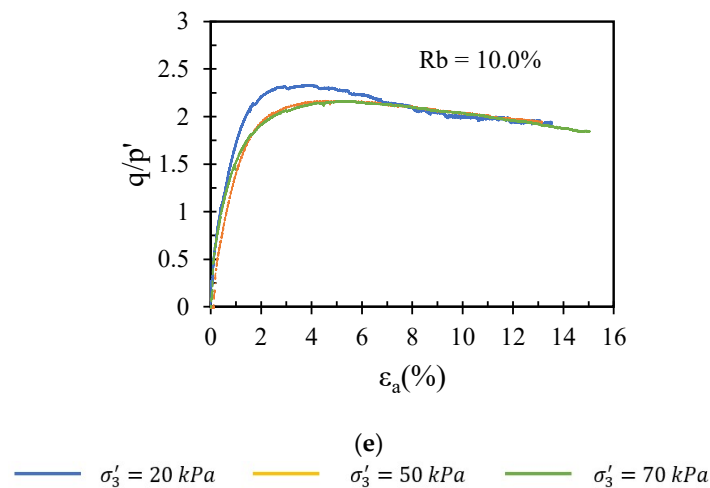


Figure 9. Monotonic triaxial compression tests' results: deviatoric stress normalized by mean effective stress (q/p') for several rubber contents: (a) 0%; (b) 2.5%; (c) 5.0%; (d) 7.5% and (e) 10.0%.

Figure 9 shows that the slag–rubber mixtures have a stress–strain behaviour typical of dense granular materials, with a peak strength followed by post-peak softening. However, it is observed that the peak of the stress–strain curve is more pronounced for a smaller quantity of rubber and a lower confining stress. The increase in the rubber content results in a reduction in the peak resistance and higher axial strain at peak, which represents a loss in stiffness. This is expected since the slag is being replaced by a more deformable material. Notwithstanding, a high residual friction angle was obtained even in the specimens with a rubber content of 10%.

To understand the effect of the rubber content on the stress–strain curves, the brittleness index, as proposed by [50] and described in Equation (2), is presented in Figure 10, assuming that the residual strength corresponds to the last measured point of the stress–strain curve at around a strain of 14%.

$$I_B = \frac{q_{peak} - q_{residual}}{q_{peak}} \quad (2)$$

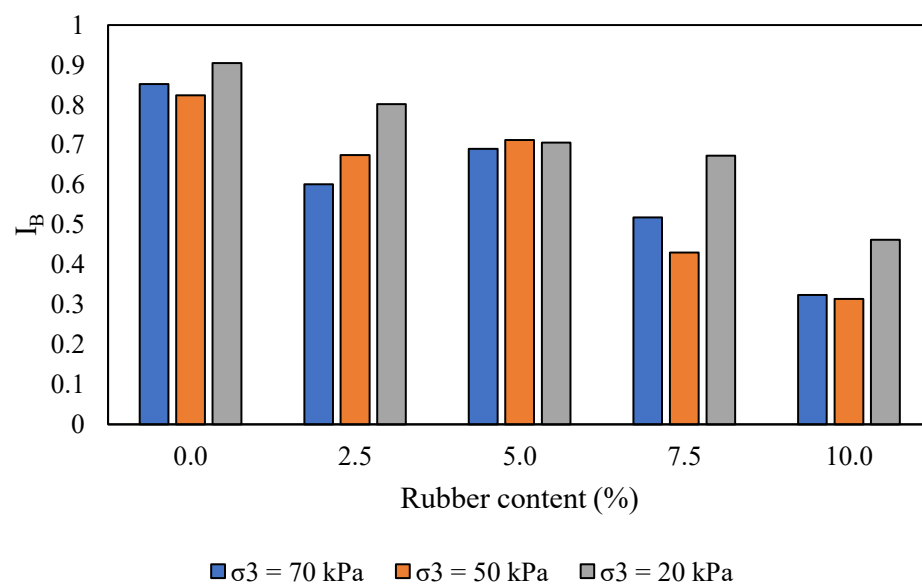


Figure 10. Brittleness index for different rubber contents and confining pressures.

As observed in Figure 10, the brittleness index, which represents the strain-softening behaviour typical of dense granular materials associated to dilatant behaviour, tends to decrease with the amount of rubber. This may be due to the residual strength that tends to be approximately similar for all rubber contents while the peak strength tends to decrease. This means that with increasing confining pressures and rubber content, the dilation is smaller and so are the brittleness index and peak strength. In granular materials, an increase in the confining pressure corresponds to a reduction in brittleness, since the confining pressure prevents dilation [51]. This is also visible in the slag–rubber mixtures with confining pressures of 20 and 50 kPa. However, for 70 kPa of confining pressure, this is not so evident.

3.3. Strength Envelope

Figure 11 presents the Mohr–Coulomb strength envelope obtained for each mixture in a deviatoric stress versus mean effective stress plot, with the corresponding peak angles of shearing resistance. The angles of shearing resistance slightly decrease with rubber contents up to $R_b = 5\%$ and then tend to stabilize at around 53° for higher rubber contents. All mixtures have high peak angles of shearing resistance, indicating that the rubber presence has a higher effect on the stiffness than the strength behaviour. This is expected due to the high particle size of the slag grains, which leads to high dilatancy angles. In Figure 11, the stress paths followed during the cyclic triaxial tests (expressed in Table 4) are also presented.

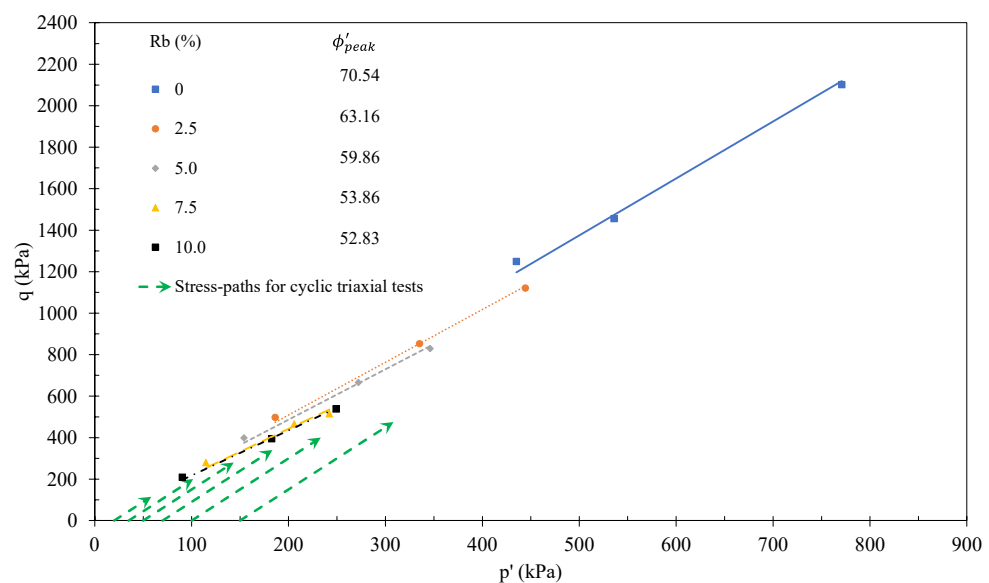


Figure 11. Strength envelope of slag and slag–rubber mixtures.

3.4. Secant Stiffness

In Figure 12, the secant stiffness modulus at 50% deviatoric stress normalized by the confining pressure is presented for different rubber contents as a function of the peak deviatoric stress. For lower rubber contents, there is a reduction in the stiffness modulus with an increase in rubber, but for rubber contents higher than 7.5%, there is a trend for secant modulus stabilization, in agreement to what is noticed for the strength. This may indicate that for rubber contents higher than 7.5%, the behaviour is probably controlled by the rubber, irrespective of the rubber content.

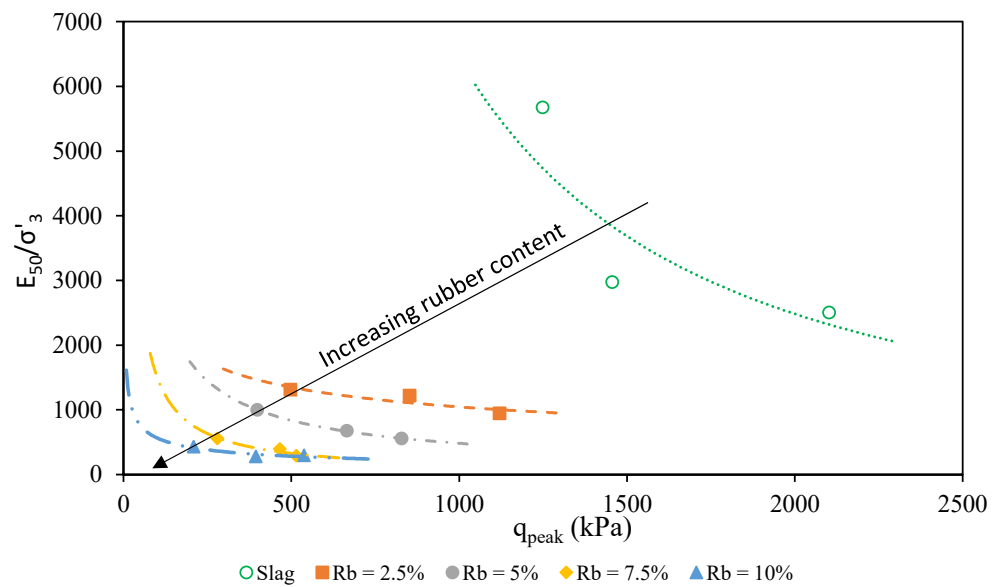


Figure 12. Evolution of the normalised secant stiffness modulus with peak deviatoric stress.

3.5. Resilient Moduli during Cyclic Loading

The resilient modulus (M_r) is defined as the unloading modulus (see Figure 13 and Equation (3)) after several cycles of repeated loading.

$$M_r = \frac{\Delta q}{\epsilon_r} = \frac{q_{max} - q_{min}}{\epsilon_r} \tag{3}$$

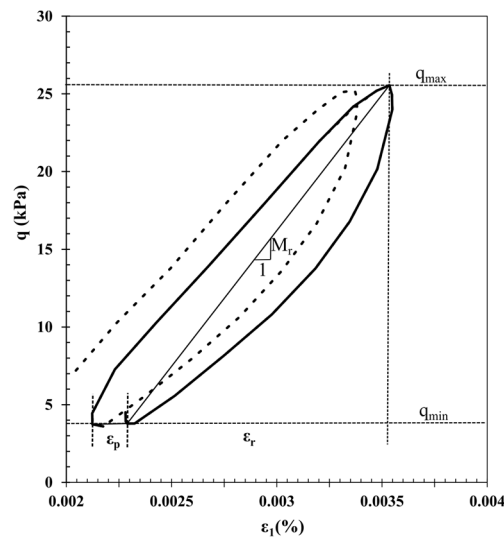


Figure 13. Schematic representation of resilient modulus definition.

Given the stress dependency of the resilient modulus in unbound granular materials, many models have been proposed to express M_r as a function of applied stress [52]. Trying to represent the increase in the resilient modulus value with increasing confining stress, Biarez [53] proposed the following equation for uniform sands:

$$M_r = k_1 \sigma_3^{k_2} \tag{4}$$

On the other hand, for clayey soils, Moossazadeh and Witczak [54] identified a greater influence of the deviatoric stress, proposing the following expression:

$$M_r = k_1 q^{k_2} \quad (5)$$

The most used model [55–57], commonly known as K- θ , is a function of the sum of principal stresses ($\theta = \sigma_1 + \sigma_2 + \sigma_3$):

$$M_r = k_1 \theta^{k_2} \quad (6)$$

Due to its simplicity, this model and its variations have been widely used in the analysis of material stiffness associated with the stress state, assuming a constant Poisson's coefficient (usually between 0.2 and 0.3 for granular materials). However, this model considers that the modulus is only a function of the sum of principal stresses, which is not reasonable, since the addition of the deviatoric stress induces more shear deformations.

In Equations (4) to (6), k_i are empirical parameters obtained from the experiments, σ'_3 is the confining stress, θ is the first invariant of stresses in axisymmetric conditions ($\theta = \sigma_1 + 2\sigma_3$), and q is the maximum deviatoric stress ($q = \sigma_1 - \sigma_3$).

In Figure 14, the resilient behaviour of the slag–rubber mixtures is presented (for rubber contents between 0% and 5%) as a function of the confining stress (Figure 14a), deviatoric stress (Figure 14b) and first invariant of stresses (Figure 14c), together with the empirical parameters that show the best adjustment to the experimental data in the basis of the minimum square fit. As expected, this figure shows a decrease in the moduli with an increase in the percentage of rubber. However, it is not the purpose of this study to increase the mechanical properties of the slag by introducing the rubber. Instead, the aim is to identify the possible applications of these mixtures containing two industrial by-products.

It is thus interesting to note that the trend that is typically seen in granular materials of increases in moduli with increasing stress levels is still observed in the slag–rubber mixtures. For this reason, the resilient moduli empirical correlations presented in Equations (4)–(6) were applied to this material. There is a strong correlation with σ'_3 and θ , but less with q , which may be expected as Equation (5) was developed for clays.

Figure 15 shows the dependency of the empirical constants (k_1 and k_2) with rubber content for the first three models. Although the models are different, the empirical constants assume similar values, having a clear relation with rubber content, with exception of k_1 from Equation (4). For k_1 there is a linear decrease with the rubber content (for Equations (5) and (6)), while k_2 tends to increase up to a rubber content of 2.5% and then stabilises.

Table 6 presents the range of resilient modulus values obtained in the cyclic triaxial tests for three rubber contents (0%, 2.5% and 5%). The successive addition of a small quantity of rubber causes a significant reduction in stiffness (approximately 3.2 and 6.6 times, respectively) at low stresses. This reduction is slightly smaller (1.72 and 2.95 times) for the higher stress level, indicating that the effect of the rubber particles' compressibility is felt mainly under low stress levels. At high stress levels, the particles are already compressed, presenting greater resistance to deformation.

Table 6. Resilient modulus values depending on the rubber content and stress level.

Stress Level		Rubber Content		
		0%	2.5%	5%
Lower stress level	$\sigma'_3 = 20$ kPa, $q = 30$ kPa	170 MPa	50 MPa	25 MPa
Higher stress level	$\sigma'_3 = 150$ kPa, $q = 475$ kPa	1000 MPa	580 MPa	340 MPa

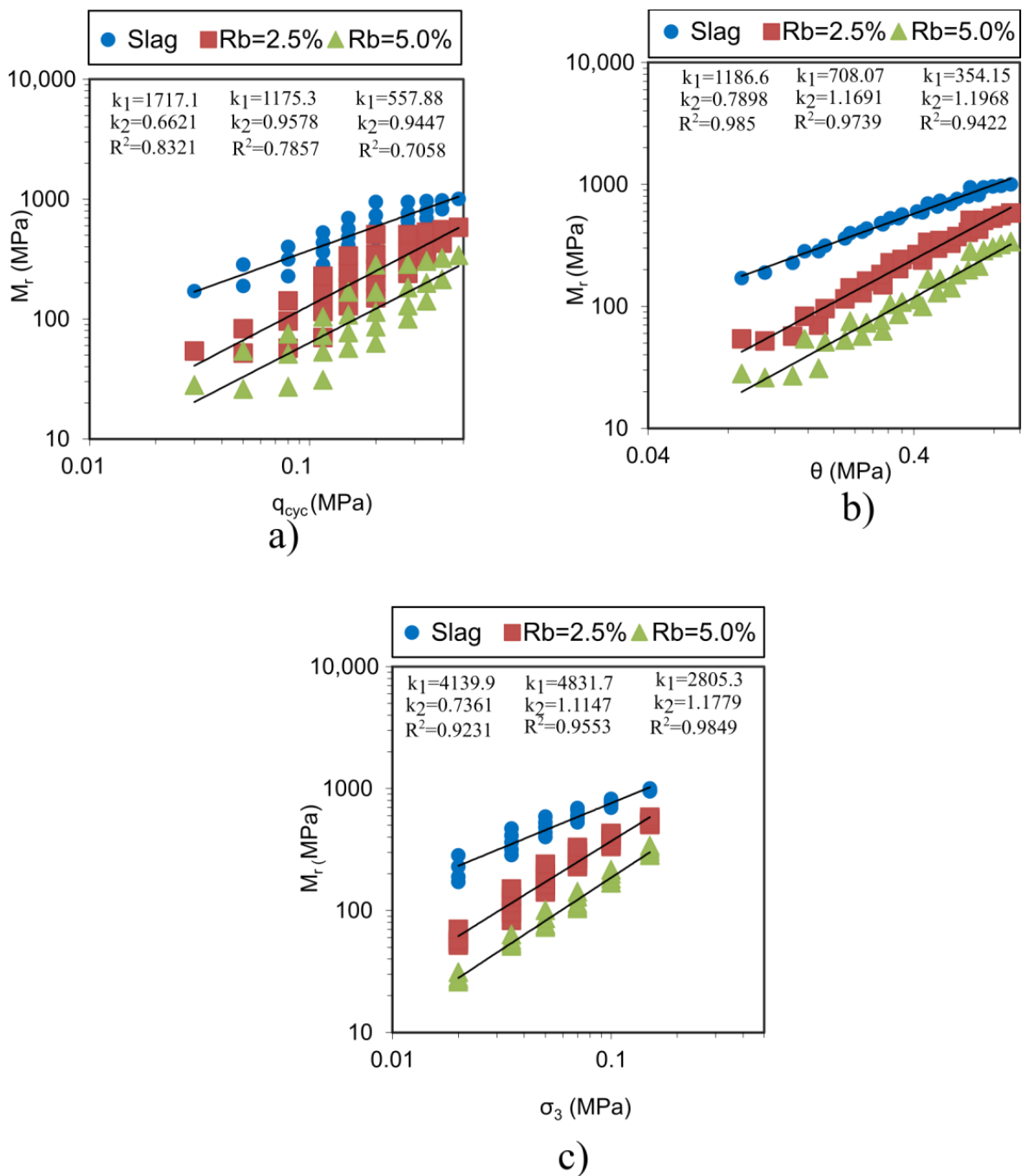


Figure 14. Resilient modulus for different percentages of rubber as a function of: (a) confining stress; (b) cyclic deviatoric stress; (c) first invariant of stresses.

According to Shahu et al. [58], the resilient modulus values required for a sub-ballast layer are around 60–100 MPa, indicating that the slag rubber mixtures studied herein have resilient moduli values acceptable for sub-ballast layers when the confining pressure is larger than 20 kPa and the rubber content is up to 2.5%.

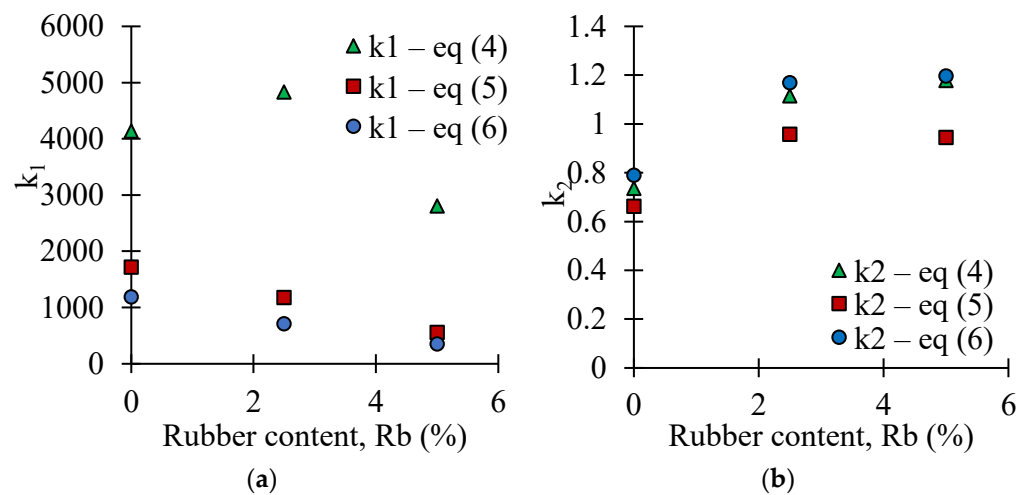


Figure 15. Empirical constants for resilient modulus models with rubber content: (a) k_1 ; (b) k_2 .

3.6. Comparison with Previous Studies

Table 7 summarises the results obtained in this study, together with data from other studies. It can be seen that the different research studies show relatively close values among the studied materials. As expected, the addition of rubber causes a decrease in the maximum dry density since rubber is a lighter material than the other aggregates. Moreover, since rubber is a more compressible material [59], it causes a decrease in the CBR and resilient modulus.

Table 7. Summary of obtained results and literature data.

References	Material	Maximum Dry Density (ρ_d) (g/cm ³)	California Bearing Ratio Test (CBR) (%)	Resilient Modulus (M_R) (MPa)	ϕ'_{peak} (°)
This study	Steel Slag + 0–5% of Rubber	2.45–2.85	80–213	25–170	60–71
Ferreira [60]	Steel furnace slag	2.43	72	127	42.5
Hidalgo-Signes et al. [26]	Granite Aggregate + 0–5% Rubber	2.17–2.32	27–154	92.8–249.6	40° (only for 0%)
Qi et al. [28]	Steel furnace slag + Coal Wash + 0–40% of Rubber Crumb	1.27–2.1	4–58	20–140	44–52
Arulrajah et al. [27]	Crushed Rock + 0–3% of Rubber	2.1–2.2	90–130	27–210	Not measured
Maghool et al. [3]	Steel furnace slag	2.43	55	198	55
Zhang et al. [61]	Granite Aggregate + 0–30% Rubber	1.6–2.0	Not measured	150–275	36–37.8

Depending on the rubber content, the values of the resilient modulus range between 20 and 249.6 MPa, while the peak angles of the shearing resistance are always high, between 40 and 71 degrees.

Comparing the results of the slag–rubber mixtures obtained in this work with the granitic aggregate–rubber mixtures found in the literature, it seems that the slag without rubber has greater resilient modulus values than natural aggregates, which is in agreement with previous studies [1] demonstrating the enhanced mechanical performance of slag particles. However, when the rubber is added, the opposite is verified, which may be associated to the interlocking of slags and rubber. This is more easily analysed when the same stress levels are compared. Hidalgo Signes et al. [26] obtained resilient modulus values ranging from 92.8 to 249.6 MPa for a confining stress of 34.5 kPa and a deviatoric of 103.4 kPa. In a similar stress state ($\sigma'_3 = 35$ kPa, $q = 115$ kPa), the mixtures analysed in this paper vary from 53 to 362 MPa for rubber contents of 5% and 0%, respectively. Zhang et al. [61] obtained resilient modulus values between 150 and 275 MPa with a confining stress of 50 kPa and a deviatoric stress of 200 kPa. For the same stress conditions, the resilient moduli of the mixtures studied in this paper vary between 86 and 529 MPa for rubber contents of 5% and 0%. However, more studies are needed to confirm this trend as it is expected that particle grain size has a major influence on the resilient moduli.

3.7. LWD Dynamic Moduli

Figure 16 presents the results of the dynamic modulus obtained in the LWD tests performed on the physical model. As observed above, the deformability modulus decreases with the increase in the rubber content. These moduli should be analysed in terms of the recommended values in the technical specifications for roads and railways. FGSV [62] provides the minimum values for the LWD modulus, which are 50 MPa on the top of the sub-ballast, 40 MPa on the top of the capping layer and 25 MPa on the top of the earthworks. In this context, the mixture with a 0% rubber content could be used as a sub-ballast layer, while the mixture with a 2.5% rubber content could be applied in the capping layer. Higher rubber contents do not seem adequate for the upper pavement layers, but these mixtures may still be used on the top of earthworks or embankments.

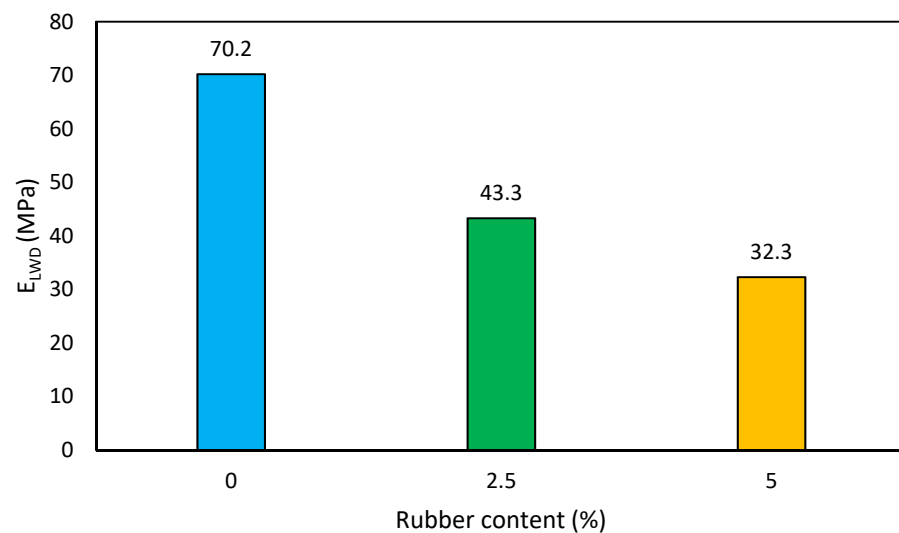


Figure 16. LWD test stiffness modulus with rubber content.

4. Conclusions

The use of industrial by-products, such as slags and rubber from end-of-life tires, in transport infrastructures has both economic and environmental benefits since it avoids the extraction of natural raw materials and provides a solution for the disposal of these materials. This paper evaluates the mechanical performance of slag–rubber mixtures for rubber contents of 0%, 2.5%, 5.0%, 7.5% and 10% to meet Brazilian, Portuguese, Australian technical specifications regarding their application in railway sub-ballast layers, capping layers or road pavement layers as bases and sub-bases. The aim is to understand under which conditions these industrial by-products can be applied in these layers without compromising the mechanical behaviour. For that purpose, laboratory tests (such as CBR, monotonic and cyclic triaxial tests) were performed in slag–rubber mixtures with a wide grain size distribution curve, while light weight deflectometer tests were performed in a physical model made with slag–rubber mixtures in which the original grain size distribution curve of the slag was used. From this study, the following conclusions were made:

- A small increase of 2.5% in rubber (from 0% to 2.5%) reduced the CBR values to half of their original value. However, for higher rubber contents, the increase of rubber has a smaller impact on the CBR values. For this reason, the CBR values obtained for mixtures with a rubber content less than 7.5% still comply to the technical recommendations available for sub-base and sub-ballast layers according to Brazilian and Portuguese technical specifications;
- For rubber contents lower than 7.5%, the secant stiffness modulus at 50% of the deviatoric stress (E_{50}) decreases with the rubber increase, but for higher rubber contents, the secant modulus tends to stabilise, in agreement with what is noticed for the angle

of shearing resistance, indicating that beyond 7.5%, the behaviour may be controlled by the rubber irrespective of the rubber content;

- The increase in rubber reduces the resilient modulus drastically, but mixtures with rubber percentages up to 5% show an acceptable performance under cyclic conditions, reaching resilient modulus values similar to those of other research studies.
- The tests performed on the physical model provided dynamic modulus values allowing for the application of slag–rubber mixtures on the capping and embankment layers of transport infrastructures for rubber contents of 2.5% and 5%, respectively.

Considering the significant economic and environmental benefits of using two industrial by-products in transport infrastructures, this work has evaluated the possible application of the different slag rubber mixtures. It was demonstrated that slag–rubber mixtures can show resilient behaviour and strength adequate for the support layers of transport infrastructures provided that the rubber content is below 5% in weight and that the slag is milled to comply with the grain size distribution ranges available in the technical specifications of the cited countries. However, more studies are being conducted to evaluate the long-term behaviour of these mixtures, namely in terms of the permanent deformation due to a large number of cyclic loads, as well as leaching tests.

Author Contributions: Conceptualization, R.A. and S.R.; methodology, R.A. and S.R.; validation, R.A., S.R., E.F. and B.G.D.; formal analysis, R.A., S.R., E.F. and B.G.D.; investigation, R.A. and S.R.; resources, A.V.d.F. and E.F.; data curation R.A., S.R. and B.G.D.; writing—original draft preparation, R.A., S.R. and B.G.D.; writing—review and editing, S.R., E.F., B.G.D. and A.V.d.F.; visualization, R.A., S.R., E.F., A.V.d.F. and B.G.D.; supervision, S.R., E.F. and A.V.d.F.; project administration, A.V.d.F.; funding acquisition, A.V.d.F. All authors have read and agreed to the published version of the manuscript.

Funding: This work was financially supported by: Base Funding—UIDB/04708/2020 of the CONSTRUCT—Instituto de I&D em Estruturas e Construções—funded by national funds through the FCT/MCTES (PIDDAC). The first author also acknowledges the support of FCT through SFRH/BD/07370/2021 grant.

Institutional Review Board Statement: Not applicable.

Informed Consent Statement: Not applicable.

Data Availability Statement: The data presented in this study is available on request from the corresponding author.

Acknowledgments: The authors would like to thank the National Laboratory for Civil Engineering (LNEC) for their support with the light weight deflectometer. The compaction equipment was also tested in the FEUP Construction Materials Testing Laboratory (LEMC), Earthquake and Structural Engineering Laboratory (LESE) and in the Professional Training Centre for Northern Civil Construction and Public Works Industry (CICCOPN), which we acknowledge gratefully. Special thanks to MEGASA for providing the slag and chemical composition, as well as GENAN for the rubber materials and information support. Caio Comini and Nelson Mica's support was very important in the preparation of the physical model. Part of the work was conducted in the framework of the TC202 National Committee of the Portuguese Geotechnical Society (SPG) 'Transportation Geotechnics', in association with the International Society for Soil Mechanics and Geotechnical Engineering (ISSMGE-TC202).

Conflicts of Interest: No potential conflict of interest was reported by the authors.

References

1. Correia, A.G.; Roque, A.J.; Ferreira, S.M.R.; Fortunato, E.; Edil, T.; Dean, S.W. Case Study to Promote the Use of Industrial Byproducts: The Relevance of Performance Tests. *J. ASTM Int.* **2012**, *9*, 1–18. [[CrossRef](#)]
2. Delgado, B.G.; da Fonseca, A.V.; Fortunato, E.; Paixão, A.; Alves, R. Geomechanical assessment of an inert steel slag aggregate as an alternative ballast material for heavy haul rail tracks. *Constr. Build. Mater.* **2021**, *279*, 1–14. [[CrossRef](#)]
3. Maghool, F.; Arulrajah, A.; Suksiripattanapong, C.; Horpibulsuk, S.; Mohajerani, A. Geotechnical properties of steel slag aggregates: Shear strength and stiffness. *Soils Found.* **2019**, *59*, 1591–1601. [[CrossRef](#)]

4. Shiha, M.; El-Badawy, S.; Gabr, A. Modeling and performance evaluation of asphalt mixtures and aggregate bases containing steel slag. *Constr. Build. Mater.* **2020**, *248*, 1–15. [[CrossRef](#)]
5. ASTM D6270; Standard Practice for Use of Scrap Tires in Civil Engineering Applications. ASTM International: West Conshohocken, PA, USA, 2020. [[CrossRef](#)]
6. Downs, L.A.; Humphrey, D.N.; Katz, L.E.; Rock, C.A. *Water Quality Effects of Using Tire Chips Below the Groundwater Table*; University of Maine: Orono, ME, USA, 1996.
7. Ferreira, V.J.; Sáez-De-Guinoa Vilaplana, A.; García-Armingol, T.; Aranda-Usón, A.; Lausín-González, C.; López-Sabirón, A.M.; Ferreira, G. Evaluation of the steel slag incorporation as coarse aggregate for road construction: Technical requirements and environmental impact assessment. *J. Clean. Prod.* **2016**, *130*, 175–186. [[CrossRef](#)]
8. Gökalp, I.; Uz, V.E.; Saltan, M.; Tutumluer, E. Technical and environmental evaluation of metallurgical slags as aggregate for sustainable pavement layer applications. *Transp. Geotech.* **2018**, *14*, 61–69. [[CrossRef](#)]
9. Mashiri, M.; Vinod, J.; Sheikh, M.N.; Tsang, H.-H. Shear strength and dilatancy behaviour of sand–tyre chip mixtures. *Soils Found.* **2015**, *55*, 517–528. [[CrossRef](#)]
10. Fu, R.; Coop, M.R.; Li, X.Q. Influence of Particle Type on the Mechanics of Sand–Rubber Mixtures. *J. Geotech. Geoenviron. Eng.* **2017**, *143*, 1–15. [[CrossRef](#)]
11. Foose, G.J.; Benson, C.H.; Bosscher, P.J. Sand Reinforced with Shredded Waste Tires. *J. Geotech. Eng.* **1996**, *122*, 760–767. [[CrossRef](#)]
12. Reddy, S.B.; Kumar, D.P.; Krishna, A.M. Evaluation of the Optimum Mixing Ratio of a Sand-Tire Chips Mixture for Geoengineering Applications. *J. Mater. Civ. Eng.* **2016**, *28*, 1–7. [[CrossRef](#)]
13. Madhusudhan, B.R.; Boominathan, A.; Banerjee, S. Factors Affecting Strength and Stiffness of Dry Sand-Rubber Tire Shred Mixtures. *Geotech. Geol. Eng.* **2019**, *37*, 2763–2780. [[CrossRef](#)]
14. Noorzad, R.; Raveshi, M. Mechanical Behavior of Waste Tire Crumbs–Sand Mixtures Determined by Triaxial Tests. *Geotech. Geol. Eng.* **2017**, *35*, 1793–1802. [[CrossRef](#)]
15. Youwai, S.; Bergado, D.T. Strength and deformation characteristics of shredded rubber tire–sand mixtures. *Can. Geotech. J.* **2003**, *40*, 254–264. [[CrossRef](#)]
16. Anastasiadis, A.; Senetakis, K.; Pitolakis, K. Small-Strain Shear Modulus and Damping Ratio of Sand-Rubber and Gravel-Rubber Mixtures. *Geotech. Geol. Eng.* **2012**, *30*, 363–382. [[CrossRef](#)]
17. Senetakis, K.; Anastasiadis, A.; Pitolakis, K. Dynamic properties of dry sand/rubber (SRM) and gravel/rubber (GRM) mixtures in a wide range of shearing strain amplitudes. *Soil Dyn. Earthq. Eng.* **2012**, *33*, 38–53. [[CrossRef](#)]
18. Nakhaei, A.; Marandi, S.; Kermani, S.S.; Bagheripour, M. Dynamic properties of granular soils mixed with granulated rubber. *Soil Dyn. Earthq. Eng.* **2012**, *43*, 124–132. [[CrossRef](#)]
19. Fernández, P.M.; Signes, C.H.; Sanchís, I.V.; Mira, D.P.; Franco, R.I. Real scale evaluation of vibration mitigation of sub-ballast layers with added tyre-derived aggregate. *Constr. Build. Mater.* **2018**, *169*, 335–346. [[CrossRef](#)]
20. Pistolas, G.A.; Anastasiadis, A.; Pitolakis, K. Dynamic Behaviour of Granular Soil Materials Mixed with Granulated Rubber: Effect of Rubber Content and Granularity on the Small-Strain Shear Modulus and Damping Ratio. *Geotech. Geol. Eng.* **2018**, *36*, 1–15. [[CrossRef](#)]
21. Esmaeili, M.; Aela, P.; Hosseini, A. Experimental assessment of cyclic behavior of sand-fouled ballast mixed with tire derived aggregates. *Soil Dyn. Earthq. Eng.* **2017**, *98*, 1–11. [[CrossRef](#)]
22. Esmaeili, M.; Zakeri, J.; Ebrahimi, H.; Sameni, M.K. Experimental study on dynamic properties of railway ballast mixed with tire derived aggregate by modal shaker test. *Adv. Mech. Eng.* **2016**, *8*, 1–13. [[CrossRef](#)]
23. Fathali, M.; Nejad, F.M.; Esmaeili, M. Influence of Tire-Derived Aggregates on the Properties of Railway Ballast Material. *J. Mater. Civ. Eng.* **2017**, *29*, 1–9. [[CrossRef](#)]
24. Guo, Y.; Markine, V.; Qiang, W.; Zhang, H.; Jing, G. Effects of crumb rubber size and percentage on degradation reduction of railway ballast. *Constr. Build. Mater.* **2019**, *212*, 210–224. [[CrossRef](#)]
25. Khoshoei, S.M.; Bak, H.M.; Abtahi, S.M.; Hejazi, S.M.; Shahbodagh, B. Experimental Investigation of the Cyclic Behavior of Steel-Slag Ballast Mixed with Tire-Derived Aggregate. *J. Mater. Civ. Eng.* **2021**, *33*, 1–11. [[CrossRef](#)]
26. Signes, C.H.; Fernández, P.M.; Perallón, E.M.; Franco, R.I. Characterisation of an unbound granular mixture with waste tyre rubber for subballast layers. *Mater. Struct.* **2015**, *48*, 3847–3861. [[CrossRef](#)]
27. Arulrajah, A.; Mohammadinia, A.; Maghool, F.; Horpibulsuk, S. Tyre derived aggregates and waste rock blends: Resilient moduli characteristics. *Constr. Build. Mater.* **2019**, *201*, 207–217. [[CrossRef](#)]
28. Qi, Y.; Indraratna, B.; Heitor, A.; Vinod, J.S. Effect of Rubber Crumbs on the Cyclic Behavior of Steel Furnace Slag and Coal Wash Mixtures. *J. Geotech. Geoenviron. Eng.* **2018**, *144*, 1–11. [[CrossRef](#)]
29. Qi, Y.; Indraratna, B. Energy-Based Approach to Assess the Performance of a Granular Matrix Consisting of Recycled Rubber, Steel-Furnace Slag, and Coal Wash. *J. Mater. Civ. Eng.* **2020**, *32*, 1–12. [[CrossRef](#)]
30. Delgado, B.G.; Da Fonseca, A.V.; Fortunato, E.; Da Motta, L.M.G. Particle morphology's influence on the rail ballast behaviour of a steel slag aggregate. *Environ. Geotech.* **2022**, *9*, 373–382. [[CrossRef](#)]
31. Paixão, A.; Fortunato, E. Abrasion evolution of steel furnace slag aggregate for railway ballast: 3D morphology analysis of scanned particles by close-range photogrammetry. *Constr. Build. Mater.* **2021**, *267*, 1–22. [[CrossRef](#)]
32. Delgado, B.G.; da Fonseca, A.V.; Fortunato, E.; Maia, P. Mechanical behavior of inert steel slag ballast for heavy haul rail track: Laboratory evaluation. *Transp. Geotech.* **2019**, *20*, 1–10. [[CrossRef](#)]

33. Rios, S.; Kowalska, M.; da Fonseca, A.V. Cyclic and Dynamic Behavior of Sand–Rubber and Clay–Rubber Mixtures. *Geotech. Geol. Eng.* **2021**, *39*, 3449–3467. [[CrossRef](#)]
34. Elshaer, M.; Ghayoomi, M.; Daniel, J.S. The role of predictive models for resilient modulus of unbound materials in pavement FWD-deflection assessment. *Road Mater. Pavement Des.* **2020**, *21*, 374–392. [[CrossRef](#)]
35. Fortunato, E. Renewal of Railway Platforms. Studies about Bearing Capacity. Ph.D. Thesis, University of Porto, Porto, Portugal, 2005.
36. Nazarian, S.; Mazari, M.; Abdallah, I.N.; Puppala, A.J.; Mohammad, L.N.; Abu-Farsakh, M.Y. *Modulus-Based Construction Specification for Compaction of Earthwork and Unbound Aggregate*; Transportation Research Board, The National Academies Press: Washington, DC, USA, 2010.
37. EN 13242:2002 + A1:2007; Aggregates for Unbound and Hydraulically Bound Materials for Use in Civil Engineering Work and Road Construction. CEN: Brussels, Belgium, 2008.
38. REFER. IT.GEO.006; Technical Characteristics of the Sub-Ballast; Technical Instruction. National Railway Network; EPE: Lisbon, Portugal, 2007.
39. Thom, N.H.; Brown, S.F. The effect of grading and density on the mechanical properties of a crushed dolomitic limestone. In Proceedings of the 14th Australian Road Research Board (ARRB) Conference, Canberra, Australia, 28 August–2 September 1998; pp. 94–100.
40. ASTM D2487; Standard Practice for Classification of Soils for Engineering Purposes (Unified Soil Classification System). ASTM International: West Conshohocken, PA, USA, 2011.
41. Fortunato, E.; Paixão, A.; Lopes, D.; Fardilha, R.; Correia, J. Laboratorial Study on Unbound Granular Materials Applied in Rail Tracks Using Cyclic Triaxial Tests. In Proceedings of the 13th National Congress on Geotechnics, Lisbon, Portugal, 17–20 April 2012. (In Portuguese).
42. Indraratna, B.; Qi, Y.; Heitor, A. Evaluating the Properties of Mixtures of Steel Furnace Slag, Coal Wash, and Rubber Crumbs Used as Subballast. *J. Mater. Civ. Eng.* **2018**, *30*, 1–9. [[CrossRef](#)]
43. Lekarp, F.; Isacsson, U. The Effects of Grading Scale on Repeated Load Triaxial Test Results. *Int. J. Pavement Eng.* **2007**, *2*, 85–101. [[CrossRef](#)]
44. CEN EN 13286-7; Unbound and hydraulically bound mixtures–Part 7: Cyclic load triaxial test for unbound mixtures. European Committee for Standardization: Brussels, Belgium, 2004.
45. Cruz, N.; Rios, S.; Fortunato, E.; Rodrigues, C.; Cruz, J.; Mateus, C.; Ramos, C. Characterization of Soil Treated With Alkali-Activated Cement in Large-Scale Specimens. *Geotech. Test. J.* **2017**, *40*, 618–629. [[CrossRef](#)]
46. ASTM D698; Standard Test Methods for Laboratory Compaction Characteristics of Soil Using Standard Effort (12 400 ft-lbf/ft³ (600 kN-m/m³)). ASTM International: West Conshohocken, PA, USA, 2021. [[CrossRef](#)]
47. Wu, Y.; Wang, X.; Shen, J.-H.; Cui, J.; Zhu, C.-Q.; Wang, X.-Z. Experimental Study on the Impact of Water Content on the Strength Parameters of Coral Gravelly Sand. *J. Mar. Sci. Eng.* **2020**, *8*, 634. [[CrossRef](#)]
48. DNIT—National Department of Transport Infrastructure. ISF-212: *Permanent Way Superstructure Project - Ballast and Subballast*; Railway Service Instruction, Ministry of Transport: Brasília, Brazil, 2015.
49. NTG, “Standard Specification for Roadworks v5.1.” Northern Territory Government of Australia. 2022; p. 368. Available online: <https://dipl.nt.gov.au/industry/technical-standards-guidelines-and-specifications/technical-specifications/roads> (accessed on 1 October 2022).
50. Towhata, I. *Geotechnical Earthquake Engineering*; Springer: Berlin/Heidelberg, Germany, 2008.
51. Chen, R.-H.; Huang, Y.-W.; Huang, F.-C. Confinement effect of geocells on sand samples under triaxial compression. *Geotext. Geomembranes* **2013**, *37*, 35–44. [[CrossRef](#)]
52. Han-Cheng, D.; Lin-Hua, H.; Lian-Heng, Z. Experimental investigation on the resilient response of unbound graded aggregate materials by using large-scale dynamic triaxial tests. *Road Mater. Pavement Des.* **2020**, *21*, 434–451. [[CrossRef](#)]
53. Biarez, J. Contribution à L’étude des Propriétés Mécaniques des sols et des Matériaux Pulvérulents. Ph.D. Thesis, Faculte des Sciences de Grenoble, Saint-Martin-d’Hères, France, 1962.
54. Moossazadeh, J.; Witczak, M. Prediction of Subgrade Moduli for Soil that Exhibits Nonlinear Behavior. *Transportation Research Record*, n. 810. 1981, pp. 9–17. Available online: <http://onlinepubs.trb.org/Onlinepubs/trr/1981/810/810-002.pdf> (accessed on 1 October 2022).
55. Seed, H.B.; Mitry, F.G.; Monismith, C.L.; Chan, C.K. Prediction of Flexible Pavement Deflections from Laboratory Repeated-Load Tests. NCHRP Report., n. 35. 1967. Available online: <https://trid.trb.org/view/104508> (accessed on 1 October 2022).
56. Brown, S.; Pell, P. An experimental investigation of the stresses, strains and deflections in a layered pavement structure subjected to dynamic loads. In Proceedings of the International Conference on the Structural Design of Asphalt Pavements, Ann Arbor, MI, USA, 7–11 August 1967.
57. Hicks, R.G.; Monismith, C.L. Factors Influencing the Resilient Response of Granular Materials. *Transp. Res. Rec.* **1971**, *345*, 15–31.
58. Shahu, J.T.; Rao, N.K. Yudhbir Parametric study of resilient response of tracks with a sub-ballast layer. *Can. Geotech. J.* **1999**, *36*, 1137–1150. [[CrossRef](#)]
59. Tasalotti, A.; Chiaro, G.; Murali, A.; Banasiak, L. Physical and Mechanical Properties of Granulated Rubber Mixed with Granular Soils—A Literature Review. *Sustainability* **2021**, *13*, 4309. [[CrossRef](#)]

60. Ferreira, S. Environmental and Mechanical Behaviour of Granular Materials. Application to National Steel Slags. Ph.D. Thesis, University of Minho, Braga, Portugal, 2010.
61. Zhang, J.; Yang, N.; Chen, X.; Hu, H.; Wang, X.; Zhang, J. Investigation of the static and dynamic characteristics of TDA-subballast mixtures. *Transp. Geotech.* **2021**, *32*, 1–14. [[CrossRef](#)]
62. FGSV: Earthworks and Foundation Engineering Task Force. Supplementary Technical Terms and Conditions of Contract and Guidelines for Earthworks in Road Construction. ZTVE-StB. 1997. Available online: <https://insitutek.com/wp-content/uploads/2014/12/Collation-of-German-Road-Rail-Standards-for-the-Light-Weight-Deflectometer-LWD.pdf> (accessed on 1 October 2022).

Disclaimer/Publisher’s Note: The statements, opinions and data contained in all publications are solely those of the individual author(s) and contributor(s) and not of MDPI and/or the editor(s). MDPI and/or the editor(s) disclaim responsibility for any injury to people or property resulting from any ideas, methods, instructions or products referred to in the content.